

---

# Rethinking Predictive Modeling for LLM Routing: When Simple kNN Beats Complex Learned Routers

---

Yang Li  
yli.ml.research@gmail.com

## Abstract

As large language models (LLMs) grow in scale and specialization, routing—selecting the best model for a given input—has become essential for efficient and effective deployment. While recent methods rely on complex learned routing strategies, their dependence on disparate training data and evaluation setups makes comparison and generalization difficult. In this work, we revisit LLM routing through the lens of simplicity. We show that a well-tuned k-Nearest Neighbors (kNN) approach not only matches but often outperforms state-of-the-art learned routers across diverse tasks. To support systematic evaluation, we introduce a suite of standardized routing benchmarks spanning instruction-following, question-answering, and reasoning tasks, as well as the first multi-modal routing dataset involving visual inputs. Our findings reveal that the locality properties of model performance in embedding space enable simple non-parametric methods to achieve strong routing decisions with lower sample complexity than parametric approaches. This challenges the prevailing trend toward sophisticated architectures and highlights the importance of thoroughly evaluating simple baselines before investing in complex solutions. To support reproducibility and further exploration, we will release all benchmarks and code upon publication.

## 1 Introduction

The proliferation of large language models (LLMs) in recent years has created an increasingly diverse ecosystem of models with varying sizes, capabilities, and specializations [1, 2, 3, 4]. As organizations and users gain access to this expanding array of models—each with different strengths, computational demands, and cost profiles—a crucial challenge has emerged: how to intelligently select the most appropriate model for a given input. This challenge, known as LLM routing, carries significant implications for both cost-effective deployment and optimal user experience [5, 6].

Current LLM routing approaches typically employ sophisticated learned policies that leverage various signals, such as model preferences [7], prompt embeddings [8], or external scoring functions [9, 10]. These methods vary in their implementation strategies—some frame routing as a selection or classification problem [10, 11, 12], while others develop predictive models to estimate utility scores of each LLM for specific inputs [13, 14]. Importantly, these diverse approaches often rely on different training datasets, evaluation protocols, and underlying assumptions, creating challenges for comparisons and raising questions about their generalizability across deployment scenarios.

While the field continues to develop increasingly complex routing solutions, we question whether such sophistication is necessary. In this paper, we take a step back and reconsider LLM routing from first principles, posing a fundamental question: *how far can we get with simple, non-parametric methods like k-Nearest Neighbors (kNN)?* Our investigation yields a surprising finding: when carefully implemented and tuned, a simple kNN-based router consistently matches or outperforms a wide range of complex learned approaches across diverse routing scenarios.

To address the evaluation inconsistency problem highlighted earlier, we introduce a standardized benchmark suite for LLM routing. This suite, derived from existing evaluation datasets, spans instruction-following, question-answering, and reasoning tasks while establishing consistent protocols and performance metrics. Our framework enables meaningful comparisons between routing approaches under identical conditions, filling a significant gap in the field.

Building upon these principles, we extend our investigation to multi-modal scenarios by developing the first benchmark for routing between vision-language models. This extension explores how routing challenges evolve when inputs span different modalities and models exhibit specialized capabilities across them. Our findings demonstrate that the simplicity advantage of kNN-based routing persists even in these more complex multi-modal scenarios, suggesting that the approach’s effectiveness generalizes beyond text-only applications.

Our results challenge the prevailing notion that sophisticated learning-based routers are necessary for high-quality LLM routing. We find that simple, robust methods grounded in existing evaluation signals often perform best—a finding consistent with Occam’s razor and reminiscent of similar discoveries in other areas of machine learning where simple baselines have proven surprisingly effective. Through theoretical analysis, we demonstrate that this effectiveness stems from the strong locality properties in embedding spaces, where semantically similar queries tend to benefit from similar models, allowing kNN approaches to achieve strong performance with lower sample complexity than parametric methods.

This work represents not just an evaluation of routing methods, but a fundamental rethinking of the approach to LLM routing in increasingly complex model ecosystems. By demonstrating the effectiveness of simple, interpretable methods, we provide both practical guidance for practitioners and theoretical insights for researchers working to advance the field. Furthermore, our findings have important implications for democratizing access to effective multi-model systems, as simpler routing methods can significantly reduce the computational and engineering overhead required to deploy sophisticated LLM-powered applications.

## 2 Background and Related Works

As the ecosystem of large language models (LLMs) becomes increasingly diverse, optimizing the trade-off between performance and computational cost has become a central research challenge. To this end, three primary strategies have emerged: ensemble methods, cascading approaches, and routing systems.

**Ensemble methods** improve robustness and answer quality by aggregating outputs from multiple LLMs. Prior works such as LLM-Blender [15], Blending [16], and Fusion [17] demonstrate that ensembling can yield strong performance across a range of tasks. However, this comes at a significant cost—ensemble methods require simultaneous inference from multiple models, leading to increased latency and computational overhead.

**Cascading approaches** aim to reduce these costs by invoking models in a sequence of increasing capability and expense. Systems like FrugalGPT [18], AutoMix [19], and Two-tier Selection [20] start with smaller models and escalate only when necessary. While this sequential design can lower the average cost, it still incurs multiple model calls for harder queries and often relies on auxiliary quality estimation mechanisms, which can introduce latency and complexity.

**Routing systems** offer a more direct and efficient alternative by selecting a single LLM to handle each query. These systems eliminate the need for multiple model calls, minimizing both cost and latency. Most routing approaches rely on performance prediction to guide model selection. Some methods predict evaluation scores or reward values for each model given an input [21, 22, 23], while others take a comparative approach by estimating win rates or preference relationships between model pairs [11, 7]. More recently, MetaLLM [13] and LLMBandit [14] frame the problem as a contextual bandit, learning routing policies that balance exploration and exploitation for model selection.

Table 1 provides an overview of existing routing approaches, categorized by their formulation, training signals, and whether they utilize support sets. This landscape illustrates the diversity of current methods, which we systematically evaluate in our work.

Table 1: Overview of existing routers.

Routers	Routing Formulation	Training Signal	Training Objective	Support Set
TensorOpera [10]	Classification	BERTsim score	Cross Entropy	No
HybridLLM [11]	Classification	BART score	Cross Entropy	No
ZOOTER [9]	Classification	Reward model	KL divergence	No
GraphRouter [12]	Classification	Evaluation metric	Cross Entropy	Yes
RouterDC [8]	Embedding Similarity	Answer correctness	Contrastive learning	No
MetaLLM [13]	Multi-armed Bandit	Online utility score	Linear reward model	No
LLMBandit [14]	Multi-armed Bandit	Online utility score	PPO policy learning	No
RouteLLM [7]	Ranking	Pairwise preference	Contrastive loss	No
Eagle [24]	Ranking	Pairwise preference	ELO calculation	Yes
ROUTOO [25]	Utility Prediction	Answer correctness	Cross Entropy	No
FORC [23]	Utility Prediction	Evaluation metric	Cross Entropy	No
Tryage [22]	Utility Prediction	Expert model losses	Divergence	No

In this work, we focus on the routing setting due to its strong efficiency potential and practical relevance. Our study highlights the surprising strength of non-parametric methods and raises important questions about the necessity and generalization ability of more complex learned routers.

### 3 Predictive LLM Routing

The goal of LLM routing is to select the most appropriate model from a set of available LLMs to process a given input query, subject to constraints such as performance, cost, or latency. Formally, let  $x$  denote a query and  $\mathcal{M} = \{m_1, m_2, \dots, m_M\}$  represent the pool of candidate models. For each  $(x, m)$  pair, we define an unknown performance score  $s(x, m)$  that captures the quality of model  $m$ 's response to query  $x$  (e.g., accuracy or reward), and a cost function  $c(x, m)$  that reflects the resource cost of invoking model  $m$  on input  $x$  (e.g., latency or compute cost, which may depend on input and response length). The objective is to select a model that maximizes utility while balancing cost:

$$m^* = \arg \max_{m \in \mathcal{M}} s(x, m) - \lambda \cdot c(x, m), \quad (1)$$

where  $\lambda$  is a user-defined trade-off parameter governing the preference for performance versus efficiency.

We study two complementary classes of routing approaches, drawing inspiration from reinforcement learning (RL): **model selection policies**, which learns a routing policy to directly predict the optimal model, and **utility prediction methods**, which estimate the score  $s(x, m)$  and cost  $c(x, m)$  for each model and select the one with the highest predicted utility. Table 1 provides an overview of existing routers mapped to these categories.

**Routing as LLM Selection** In this formulation, routing is framed as a direct model selection problem: given an input  $x$ , the router learns a policy  $\pi(x)$  that maps queries to models, aiming to predict the optimal choice  $m^*$ . This perspective is analogous to policy gradient methods in RL, where an agent learns to output actions directly without explicitly estimating the value of all alternatives.

The policy  $\pi(x)$  can be parametrized in various ways. Several approaches structure it as a classifier, with gold routing labels derived from preference data [7], reward scores [10], or thresholded evaluation metrics [11]. Other methods parametrize the policy as a distance measure between query and model embeddings, formulating the problem as an embedding learning task trained using contrastive objectives [8]. A third line of work frames routing as a contextual bandit problem, directly learning routing policies from online feedback [13, 14]. These approaches differ in their learning objectives and adaptation capabilities, but all ultimately aim to map inputs to optimal model selections.

**Routing as Utility Prediction** Alternatively, routing can be framed as a utility estimation problem: for each input  $x$  and candidate model  $m$ , the system predicts a scalar utility score  $\hat{u}(x, m) = \hat{s}(x, m) - \lambda \cdot \hat{c}(x, m)$ , where  $\hat{s}(x, m)$  and  $\hat{c}(x, m)$  are predicted score and cost. Routing is then performed by selecting the model with the highest predicted utility.

This formulation directly parallels  $Q$ -learning in reinforcement learning, where the  $Q$ -function  $Q(x, a)$  estimates the expected return of taking action  $a$  in state  $x$ , and the policy selects the action with the highest  $Q$ -value. In the LLM routing context, "actions" correspond to candidate models, and utility predictors serve as the  $Q$ -function. This approach enables more nuanced reasoning over model selection and naturally accommodates complex scenarios involving multi-objective tradeoffs.

By explicitly estimating both performance and cost dimensions, utility prediction provides a flexible framework for balancing quality and efficiency in diverse deployment settings.

**Leverage Support Sets for Enhanced Routing** Beyond direct policy learning and utility prediction, routing can be enhanced by considering each query within its neighborhood context. In this approach, a query  $x$  is routed by leveraging a support set  $\mathcal{D}_{\text{support}} = (x_i, m, s(x_i, m), c(x_i, m))$  that captures performance scores and computational costs for semantically similar prompts  $x_i$ , providing valuable contextual signals about how different models perform on related inputs.

Both the model selection and utility prediction frameworks described earlier can incorporate support sets. Non-parametric methods like  $k$ -Nearest Neighbors (kNN) estimate  $s(x, m)$  and  $c(x, m)$  by retrieving similar inputs  $x_i$  from  $\mathcal{D}_{\text{support}}$  and aggregating their recorded outcomes. Meanwhile, parametric routers can be designed to process both the target query and its neighbors, enabling them to learn from local performance-cost landscapes rather than treating each query in isolation.

This contextual approach bridges the gap between instance-level prediction and dataset-level routing patterns. It enables practical, test-time adaptive routing that can respond to distribution shifts without requiring complete retraining. In our experiments, we find that support set utilization provides substantial benefits across different routing architectures, with even simple kNN-based methods achieving surprisingly strong performance. This finding suggests that the local structure of model performance and cost patterns contains rich signal that sophisticated routers can exploit for more accurate and efficient model selection.

## 4 Routing Benchmarks

To enable systematic evaluation of routing approaches, we develop standardized benchmarks that address the inconsistent evaluation protocols which have hindered meaningful comparisons between routing methods.

### 4.1 Text-Based Routing Benchmarks

While RouterBench [26] provides a valuable starting point for routing evaluation with 11 LLMs across 6 tasks, its limited model pool constrains applicability to diverse real-world scenarios. To address this limitation, we construct a more comprehensive benchmark incorporating a broader range of models and tasks from established evaluation frameworks.

Our benchmark leverages three widely-used LLM evaluation leaderboards: AlpacaEval [27], Open LLM Leaderboard v2 [28], and HELM-Lite [29]. From each leaderboard, we select three model families (e.g., OpenAI GPT series, Google Gemini series), with multiple variants per family to represent practical routing scenarios. The performance scores  $s(x, m)$  are derived directly from the evaluation metrics reported in each respective leaderboard, while the costs  $c(x, m)$  are calculated using the actual pricing of each API, based on input and output token counts. For detailed benchmark construction, model selection criteria, and scoring methodology, please refer to Appendix B.

### 4.2 Vision-Language Routing Benchmarks

To address routing challenges in the increasingly important multi-modal domain, we introduce the first benchmark for routing between vision-language models. Our benchmark builds upon vHELM [30], a comprehensive evaluation framework that systematically assesses capabilities across visual understanding, reasoning, and instruction following.

We incorporate leading multi-modal models from Claude and OpenAI’s model families, selecting variants that represent different performance-cost tradeoffs. For evaluation, we curate five diverse datasets focusing on visual question answering and visual reasoning tasks, carefully chosen to represent varying levels of complexity and different visual understanding requirements. Detailed information about model selection, dataset characteristics, and evaluation metrics is provided in Appendix B.

This benchmark enables evaluation of how routing approaches handle multi-modal inputs, where optimal model selection depends not only on the text query but also on visual content characteristics, image quality, and the specific interplay between visual and textual components of the task.

Table 2: AUC scores on a range of text routing benchmarks. All methods predict utility scores to inform routing decisions. Higher is better.

	OpenAI	AlpacaEval Claude	Mistral	OpenAI	HELM-Lite Claude	Google	LLaMA3	OpenLLM Qwen2.5	Yi1.5	RouterBench	Avg
Oracle	63.17	52.98	34.69	64.30	63.75	66.74	64.11	83.32	64.12	91.91	64.91
Random	36.47	34.56	27.76	48.94	41.89	45.15	37.86	41.98	33.94	54.93	40.35
kNN (k=10)	57.33	52.82	34.27	53.93	52.66	50.92	41.45	39.67	34.98	74.22	49.23
kNN (k=100)	57.38	52.77	<b>34.26</b>	54.73	53.40	52.18	48.98	56.18	39.74	77.22	52.68
Linear	<b>57.60</b>	<b>52.84</b>	<u>34.26</u>	<b>55.61</b>	<u>53.54</u>	<b>52.64</b>	48.94	<b>56.46</b>	<u>41.83</u>	<b>77.68</b>	<b>53.14</b>
Linear (MF)	56.85	52.08	33.76	55.31	53.40	51.93	48.94	55.91	<b>41.88</b>	77.27	52.73
MLP	55.50	51.29	32.18	54.43	50.82	51.51	48.52	54.62	41.19	77.08	51.71
MLP (MF)	<u>57.50</u>	<u>52.84</u>	34.20	<u>55.60</u>	53.21	51.46	48.71	<u>56.21</u>	41.63	77.40	<u>52.88</u>
Graph (k=10)	55.66	45.64	31.50	53.34	45.19	50.45	40.06	54.99	33.62	76.24	48.67
Graph (k=100)	57.37	51.84	32.25	52.70	51.89	51.41	<b>49.10</b>	55.24	39.52	76.87	51.82
Attn (k=10)	54.43	45.12	26.52	53.07	52.35	51.89	41.09	48.00	34.58	73.53	48.06
Attn (k=100)	55.29	52.49	27.94	52.23	52.12	50.61	45.12	56.03	32.65	77.37	50.18
D-Attn (k=10)	54.50	44.62	29.34	53.31	50.17	51.38	39.54	32.05	34.81	74.40	46.41
D-Attn (k=100)	57.17	52.77	24.45	51.49	49.43	51.82	<u>49.04</u>	23.90	34.92	<u>77.48</u>	47.25

Table 3: Utility scores on a range of text routing benchmarks. All methods directly select the optimal routing model without explicitly estimating the utility scores. Scores are averaged over 3 preference settings. Higher is better.

	OpenAI	AlpacaEval Claude	Mistral	OpenAI	HELM-Lite Claude	Google	LLaMA3	OpenLLM Qwen2.5	Yi1.5	RouterBench	Avg
kNN (k=10)	38.32	42.04	23.72	<u>49.75</u>	<b>44.85</b>	<b>49.48</b>	37.85	<u>25.61</u>	32.82	53.07	39.75
kNN (k=100)	37.89	43.99	23.88	48.93	41.86	48.63	37.56	22.61	32.09	52.36	38.98
Linear	<b>54.61</b>	<b>51.14</b>	<b>30.96</b>	48.53	42.13	48.69	38.43	24.38	32.11	52.36	42.33
Linear (MF)	54.54	<u>51.14</u>	<u>30.96</u>	48.59	42.57	48.73	38.57	24.82	32.15	52.36	42.44
MLP	50.81	51.14	30.52	49.30	<b>45.37</b>	48.95	<u>39.11</u>	<b>26.20</b>	33.30	53.80	42.85
MLP (MF)	<b>54.71</b>	51.14	30.96	48.60	43.55	48.72	38.58	24.62	32.24	52.36	42.55
Graph (k=10)	54.52	51.14	30.95	48.84	43.11	48.55	38.49	24.72	32.12	52.73	42.52
Graph (k=100)	54.61	51.14	30.96	<u>50.47</u>	44.62	<b>50.72</b>	37.41	21.69	32.09	52.28	42.60
Attn (k=10)	54.08	51.14	30.91	48.45	42.08	48.04	38.86	24.85	33.76	53.74	42.59
Attn (k=100)	54.04	51.14	30.96	49.13	44.31	49.17	38.51	23.42	33.93	<u>54.43</u>	<u>42.90</u>
D-Attn (k=10)	53.84	51.14	30.91	49.29	42.06	48.33	<b>39.31</b>	25.41	<b>37.24</b>	<b>55.58</b>	<b>43.31</b>
D-Attn (k=100)	53.55	51.14	30.96	48.95	40.76	48.60	37.95	23.94	<u>34.44</u>	52.90	42.32

### 4.3 Evaluation Protocol

To systematically evaluate routing approaches with different objectives, we develop distinct evaluation protocols for utility prediction and model selection approaches:

**Utility Prediction Evaluation** These methods explicitly predict performance scores and costs, allowing us to trace the complete Pareto front by varying the trade-off parameter  $\lambda$  across a wide range. We assess router effectiveness by measuring the area under the curve (AUC) of the non-decreasing convex hull in the cost-performance space. This metric comprehensively captures a router's ability to balance performance and cost across the entire spectrum of preference settings, with higher AUC indicating better overall routing decisions. We normalize score and cost values so that the maximum AUC score is 100. Additional implementation details about the AUC calculation methodology are provided in Appendix B.

**Selection-Based Evaluation** These methods directly map queries to models without explicit utility scores, making construction of a full Pareto front challenging. We therefore evaluate these routers at three distinct cost-performance preferences and report the average utility scores across them. To enable consistent comparison across benchmarks with different cost scales, we normalize the trade-off parameter using  $c_{\max}$ , the maximum cost in each routing benchmark:

- **Low-cost preference** ( $\lambda = 1.0/c_{\max}$ ): Heavily prioritizes efficiency while maintaining minimum performance requirements
- **Balanced preference** ( $\lambda = 0.5/c_{\max}$ ): Balances performance and normalized cost
- **High-performance preference** ( $\lambda = 0.1/c_{\max}$ ): Prioritizes response quality with reduced emphasis on efficiency

For both evaluation approaches, we report performance relative to two reference points: (1) an oracle router with perfect knowledge of each model's performance and cost on each query, representing the theoretical upper bound, and (2) a random routing baseline that selects models uniformly at random, establishing a lower bound. This normalized comparison framework enables precise quantification of how closely each routing approach approximates optimal routing decisions across preference settings.

## 5 Routing Approaches

Building on our benchmarking framework, we evaluate a comprehensive set of routing approaches ranging from simple non-parametric methods to sophisticated neural architectures. We organize these approaches into two categories based on their output formulation: utility prediction models that estimate performance scores and costs, and model selection approaches that directly classify queries to specific models. While these categories differ in their output space, they share the same input representations and underlying model architectures.

**kNN Router:** A simple yet effective approach that routes queries by retrieving the  $k$  most similar examples from a training set and aggregating their performance outcomes. For utility prediction, it averages the observed scores and costs from neighbors; for model selection, it uses majority voting among the top-performing models for similar queries. We explore various values of  $k$  to optimize retrieval quality.

**Linear Router:** Employs linear regression (for utility prediction) or logistic regression (for model selection) over query embeddings, providing a simple baseline that captures linear relationships between query features and routing decisions.

**Linear Matrix Factorization (MF) Router:** Inspired by RouteLLM [7], this approach assigns a learnable embedding to each model and predicts utility scores or routing decisions through linear operations on the multiplication of prompt embeddings and model embeddings. This captures the interaction between query characteristics and model capabilities.

**MLP Router:** A feed-forward network with multiple hidden layers that learns non-linear mappings between query embeddings and routing outcomes, balancing expressiveness with efficiency.

**MLP Matrix Factorization (MF) Router:** An extension of the Linear MF approach where the interaction between prompt and model embeddings is processed through a multi-layer perceptron, allowing for more complex, non-linear interactions between query features and model attributes.

**Graph Router:** Inspired by GraphRouter [12], we represent the routing problem as a bipartite graph where queries and models form nodes, with query-to-model edges representing utility scores. This approach leverages graph neural networks to capture complex relationships between similar queries and model performance patterns.

**Attentive Router:** We propose to use permutation-invariant attention modules to capture correlations between support examples, which represent sets of prompt-utility pairs. A cross-attention mechanism between the target prompt and the support examples then aggregates these representations to predict utilities or make selection decisions.

**Double Attentive Router:** An enhanced version of the Attentive Router that additionally models dependencies across candidate models using a second attention mechanism. This allows the router to capture not only similarities between queries but also relationships between different models’ performance characteristics on related inputs.

For all approaches, we use consistent query representations based on embeddings from a pre-trained language model (for text-only routing) or a vision-language model (for multi-modal routing). This ensures fair comparison across different architectures while isolating the impact of the routing algorithm itself. Implementation details, hyperparameter settings, and training protocols for each approach are provided in Appendix C.

## 6 Quantitative Results

In this section, we present a comprehensive evaluation of diverse routing approaches across both model selection and utility prediction formulations. For textual queries, we use BERT embeddings [31] to represent the input text, while for multi-modal queries, we employ VLM2Vec [32] to extract unified representations of image-text pairs. This consistent representation approach ensures fair comparison across different routing methods. We further analyze the impact of alternative embedding models in ablation studies.

Tables 2 and 3 present the performance of various routing approaches on our text-based benchmarks. The utility prediction models are evaluated using AUC of the Pareto front, while model selection approaches are assessed at three distinct preferences representing different cost-performance tradeoffs.

Table 4: AUC scores for vision language benchmark using utility prediction routing. Higher is better.

	Blink		Flickr30k		MathVista		MME		MMMU		Avg
	OpenAI	Claude									
Oracle	98.53	92.97	78.00	73.91	89.30	63.66	97.79	90.17	92.30	80.28	85.69
Random	71.82	57.72	54.12	49.50	52.91	36.96	75.21	52.05	64.47	47.76	56.25
kNN (k=10)	83.91	77.47	59.29	61.41	65.88	49.57	90.84	84.52	75.04	58.26	70.62
kNN (k=100)	84.79	<b>78.34</b>	58.89	61.16	<b>72.96</b>	50.29	90.84	84.56	<b>78.11</b>	61.27	<b>72.12</b>
Linear	<b>85.48</b>	77.05	59.42	<b>61.69</b>	70.85	50.28	91.29	<b>85.19</b>	75.05	60.54	71.68
Linear (MF)	84.62	76.76	58.82	61.30	64.46	48.20	<b>92.19</b>	84.51	71.61	60.16	70.26
MLP	78.86	73.45	59.50	58.87	60.20	48.89	91.96	83.27	68.12	57.95	68.11
MLP (MF)	<b>84.96</b>	77.72	<b>60.29</b>	<b>61.61</b>	64.45	49.61	91.29	<b>85.62</b>	74.66	61.67	71.19
Graph (k=10)	83.55	76.45	58.66	58.34	64.48	44.71	90.79	84.02	75.04	<b>62.04</b>	69.81
Graph (k=100)	84.79	<b>78.65</b>	58.56	61.40	70.85	48.22	91.06	84.56	77.73	61.67	<b>71.75</b>
Attn (k=10)	84.08	77.14	58.31	58.29	66.57	46.10	91.06	84.75	73.87	58.26	69.84
Attn (k=100)	84.95	78.16	58.59	54.42	<b>71.54</b>	<b>50.97</b>	90.84	84.59	<b>79.26</b>	61.29	71.46
D-Attn (k=10)	83.56	76.99	<b>59.90</b>	59.37	67.27	48.87	90.82	84.75	73.80	58.28	70.36
D-Attn (k=100)	84.79	78.32	58.72	51.93	70.12	<b>50.97</b>	89.87	84.59	73.41	61.28	70.40

Table 5: Utility scores for vision language benchmark using selection based routing. Higher is better.

	Blink		Flickr30k		MathVista		MME		MMMU		Avg
	OpenAI	Claude									
kNN (k=10)	60.42	71.13	<b>56.88</b>	47.50	34.48	24.69	77.41	67.74	52.08	49.53	54.19
kNN (k=100)	54.57	71.13	56.37	<b>47.52</b>	23.39	24.23	73.79	67.74	46.35	49.28	51.44
Linear	57.01	71.13	56.37	51.06	23.39	24.92	72.17	70.92	46.35	49.28	52.26
Linear (MF)	63.96	71.13	56.37	46.42	32.60	30.24	77.95	74.59	46.73	50.40	55.04
MLP	<b>65.96</b>	<b>73.52</b>	56.62	51.51	<b>42.46</b>	32.82	74.01	78.24	<b>54.35</b>	<b>52.24</b>	<b>58.17</b>
MLP (MF)	<b>65.35</b>	71.13	56.37	46.32	23.39	33.07	75.86	76.96	46.35	49.28	54.41
Graph (k=10)	54.80	71.07	56.37	48.69	32.11	24.70	73.09	72.60	46.22	49.12	52.88
Graph (k=100)	58.06	71.70	54.68	53.99	33.63	33.06	69.17	76.47	45.74	<b>51.84</b>	54.83
Attn (k=10)	62.01	71.30	<b>56.88</b>	<b>56.42</b>	39.10	28.21	<b>77.56</b>	<b>82.39</b>	<b>54.22</b>	51.53	<b>57.96</b>
Attn (k=100)	59.34	<b>71.46</b>	<b>56.65</b>	53.39	<b>41.61</b>	<b>33.87</b>	73.54	78.89	46.12	49.52	56.44
D-Attn (k=10)	60.16	<b>70.32</b>	55.29	<b>56.19</b>	30.42	29.75	<b>78.53</b>	<b>83.75</b>	47.71	51.27	56.34
D-Attn (k=100)	59.55	71.42	53.88	52.36	29.72	<b>48.46</b>	73.83	78.46	49.10	50.04	56.68

Our results reveal several key insights:

**kNN routers achieve remarkably strong performance**, often matching or outperforming sophisticated neural approaches. For example, in the utility prediction setting, kNN with  $k=100$  achieves an average AUC score of 52.68 across all benchmarks, competitive with more complex approaches like MLP (51.71) and Graph Neural Networks (51.82).

**Simple parametric models are competitive.** Linear models achieve strong performance (average AUC of 53.14 in utility prediction), showing that complex architectures may not be necessary for effective routing.

**Model families exhibit consistent patterns.** The relative performance of routing approaches is fairly consistent across model families (OpenAI, Claude, etc.) within the same benchmark, suggesting that routing strategies generalize across different model architectures.

**Support set size matters.** In most cases, increasing  $k$  from 10 to 100 improves performance, highlighting the importance of sufficient neighborhood context for effective routing decisions.

**Performance varies with task complexity.** All routers achieve higher scores on some benchmarks (like RouterBench) than others (like OpenLLM), reflecting the inherent difficulty of the tasks.

Table 4 and Table 5 show the performance of routing approaches on our multi-modal benchmarks. The results reveal both similarities and differences compared to text-only routing:

**kNN maintains strong performance in multi-modal settings.** In the utility prediction formulation, kNN with  $k=100$  achieves a remarkable average AUC of 72.12, outperforming most neural approaches.

**Selection-based routing shows higher variance.** When routers directly predict the optimal model rather than estimating utilities, performance exhibits greater sensitivity to router architecture and hyperparameters, suggesting that multi-modal routing benefits from more careful router design in this formulation.

**Attention mechanisms show promise.** Attention-based architectures perform well on multi-modal data, with Double-Attentive routers achieving strong performance on complex tasks like MME, likely due to their ability to model relationships between visual and textual features.

Table 6: Ablation study on prompt embedding models.

	Arcc	GSM	MBPP	MMLU	Hellaswag	Winogrande	Avg	
BERT Embedding	kNN (k=10)	88.15	63.82	60.16	73.91	87.93	71.35	74.22
	kNN (k=100)	91.80	64.72	58.67	80.81	89.39	77.91	77.22
	Linear	92.27	65.50	60.76	81.05	87.87	78.63	<b>77.68</b>
	Linear (MF)	91.80	64.55	60.08	80.91	88.07	78.18	77.27
	MLP	91.78	65.03	59.35	80.22	87.85	78.22	77.08
	MLP (MF)	91.70	65.38	60.05	80.94	87.85	78.50	77.40
	Graph (k=10)	91.70	62.23	56.36	80.76	87.89	78.52	76.24
	Graph (k=100)	91.39	62.76	59.38	80.88	87.89	78.93	76.87
	Attn (k=10)	89.49	62.08	56.36	72.12	87.88	73.26	73.53
	Attn (k=100)	91.63	64.07	60.85	81.01	87.86	78.82	77.37
	D-Attn (k=10)	89.43	62.51	58.67	74.15	87.91	73.72	74.40
	D-Attn (k=100)	91.67	64.48	60.14	80.71	89.40	78.46	77.48
SFR Embedding	kNN (k=10)	88.08	63.88	61.18	74.61	84.78	73.08	74.27
	kNN (k=100)	91.33	64.95	62.22	80.94	89.08	77.76	77.71
	Linear	92.02	65.60	64.68	80.30	89.41	78.42	<b>78.41</b>
	Linear (MF)	90.80	64.71	61.72	80.01	89.43	78.62	77.55
	MLP	90.05	62.92	63.91	80.43	87.75	77.04	77.02
	MLP (MF)	91.86	65.16	64.64	80.67	89.42	78.43	78.36
	Graph (k=10)	91.04	59.62	56.37	80.92	87.97	78.77	75.78
	Graph (k=100)	91.45	61.52	60.95	81.01	88.95	78.56	77.07
	Attn (k=10)	88.13	62.13	57.10	76.56	86.56	74.18	74.11
	Attn (k=100)	91.32	64.24	60.11	80.97	89.04	78.47	77.36
	D-Attn (k=10)	88.16	62.41	56.24	76.48	86.68	73.38	73.89
	D-Attn (k=100)	91.11	64.34	59.33	81.02	89.18	78.57	77.26

Table 6 presents an ablation study comparing different embedding models for routing. Our analysis shows that:

**Embedding quality impacts routing performance.** Switching from BERT to SFR embeddings offers modest but consistent improvements across most routing architectures, with the largest gains observed for linear and MLP models.

**Embeddings impact all approaches similarly.** Both simple and complex routing methods achieve comparable performance across different embedding types, further reinforcing that sophisticated architectures may not offer significant advantages when using well-designed representations.

**The choice of  $k$  remains important regardless of embedding quality.** For both embedding types, increasing the neighborhood size consistently improves performance, confirming the importance of sufficient neighborhood context.

Overall, our quantitative results strongly suggest that well-tuned kNN-based routers, combined with high-quality query embeddings, offer a compelling alternative to complex learned routing approaches. The strong performance of simple methods across diverse benchmarks challenges the prevailing assumption that sophisticated architectures are necessary for effective LLM routing.

## 7 Theoretical Analysis

In this section, we develop a theoretical framework to explain why simple kNN-based routers often match or outperform more complex learned routers. Our analysis addresses an important question: under what conditions does the local structure of the query-performance space provide sufficient signal for effective routing?

**Local Structure of Model Performance** We begin by formalizing the locality property of model performance in the embedding space:

**Definition 1** ( $\delta$ -Locality). *Given a query embedding space  $\mathcal{X}$ , utility function  $u(x, m)$ , and the distance function  $d(\cdot, \cdot)$ , model performance exhibits  $\delta$ -locality if for any two queries  $x_1$  and  $x_2$ :*

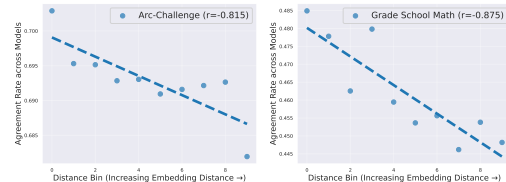


Figure 1: As the embedding distance between prompt pairs increases, the agreement between their model performance scores decreases, demonstrating the locality property in the prompt-performance space.

$d(x_1, x_2) < \delta \implies |u(x_1, m) - u(x_2, m)| < \epsilon(\delta)$ , where  $\epsilon(\delta)$  is a monotonically increasing function with  $\epsilon(0) = 0$ .

This definition captures the intuition that semantically similar queries should yield similar performance from the same model. Our empirical results in Fig. 1 suggest that current embedding spaces exhibit strong locality properties for routing.

**Sample Complexity Advantage** We now show that kNN routers benefit from lower sample complexity compared to parametric models:

**Theorem 1.** *For a query distribution  $\mathcal{D}$  with  $\delta$ -locality in utility space:*

- (a) *A kNN router requires a training sample size of  $\Theta\left(\frac{C_{\mathcal{X},d}}{\delta^d} \cdot \log\left(\frac{1}{\alpha}\right)\right)$  to achieve expected regret  $O(\epsilon(\delta))$  with probability  $1 - \alpha$ , where  $d$  is the intrinsic dimension of the embedding space and  $C_{\mathcal{X},d}$  is a constant depending on the space.*
- (b) *A parametric router with  $L$  Lipschitz-continuous layers requires a training sample size of  $\Omega(L/\epsilon(\delta)^2)$  to achieve the same regret bound.*

When the embedding space has a low intrinsic dimension  $d$  (which is often the case for well-designed embedding spaces), and  $\epsilon(\delta)$  decreases rapidly with  $\delta$  (strong locality property), the kNN router requires significantly fewer training samples than a parametric router to achieve the same regret bound. The full proof is provided in Appendix E.

## 8 Discussion and Conclusion

This paper presents a systematic re-examination of LLM routing approaches, comparing simple non-parametric methods against complex learned routers across standardized benchmarks for both text-only and multi-modal routing scenarios. We introduced comprehensive routing benchmarks spanning instruction-following, question-answering, reasoning tasks, and multi-modal inputs. We evaluated a spectrum of routing approaches—from simple kNN methods to sophisticated neural architectures—using consistent protocols that enable fair comparisons across different preference settings and cost-performance trade-offs. Our investigation revealed that well-tuned kNN-based routers consistently match or outperform more sophisticated approaches across diverse routing scenarios. This effectiveness stems from the strong locality properties in embedding spaces, where semantically similar queries benefit from similar models. Our theoretical analysis shows that kNN routers require fewer samples to achieve low regret. These findings challenge the prevailing trend toward complex routing architectures and suggest that practitioners should thoroughly evaluate simple baselines before investing in sophisticated solutions.

Several promising areas merit further exploration:

**Dynamic Adaptation:** While our study focused on static routing, kNN approaches enable straightforward online updates by incorporating new examples into the support set—combining simplicity with adaptability.

**Alternative Signals:** Our benchmarks used direct evaluation metrics as routing signals. Investigating how simple routers perform with alternative training signals (reward models, preferences) remains an important direction.

**Embedding Optimization:** Standard pre-trained embeddings proved surprisingly effective, but specialized embedding learning could further enhance routing performance, particularly where locality properties are weaker.

**Batch Routing:** Extending kNN approaches to batch routing with global computational constraints presents an interesting practical challenge.

**Generalization:** Further investigating the generalization capabilities of simple routers to new models, prompts, and unseen tasks would strengthen our understanding of when simplicity is sufficient.

As the LLM ecosystem continues to diversify, our findings indicate that simple, robust approaches deserve serious consideration in practical multi-model systems. The effectiveness of kNN routing reinforces an important principle in machine learning system design: complex solutions should be justified by meaningful performance improvements over simple baselines.

## References

- [1] Gemini Team, Rohan Anil, Sebastian Borgeaud, Jean-Baptiste Alayrac, Jiahui Yu, Radu Soricut, Johan Schalkwyk, Andrew M Dai, Anja Hauth, Katie Millican, et al. Gemini: a family of highly capable multimodal models. *arXiv preprint arXiv:2312.11805*, 2023.
- [2] Aaron Jaech, Adam Kalai, Adam Lerer, Adam Richardson, Ahmed El-Kishky, Aiden Low, Alec Helyar, Aleksander Madry, Alex Beutel, Alex Carney, et al. Openai o1 system card. *arXiv preprint arXiv:2412.16720*, 2024.
- [3] Daya Guo, Dejian Yang, Haowei Zhang, Junxiao Song, Ruoyu Zhang, Runxin Xu, Qihao Zhu, Shirong Ma, Peiyi Wang, Xiao Bi, et al. Deepseek-r1: Incentivizing reasoning capability in llms via reinforcement learning. *arXiv preprint arXiv:2501.12948*, 2025.
- [4] An Yang, Baosong Yang, Beichen Zhang, Binyuan Hui, Bo Zheng, Bowen Yu, Chengyuan Li, Dayiheng Liu, Fei Huang, Haoran Wei, et al. Qwen2. 5 technical report. *arXiv preprint arXiv:2412.15115*, 2024.
- [5] Clovis Varangot-Reille, Christophe Bouvard, Antoine Gourru, Mathieu Ciancone, Marion Schaeffer, and François Jacquenet. Doing more with less—implementing routing strategies in large language model-based systems: An extended survey. *arXiv preprint arXiv:2502.00409*, 2025.
- [6] Zhipun Chen, Jingzheng Li, Pengpeng Chen, Zhioran Li, Kai Sun, Yuankai Luo, Qianren Mao, Dingqi Yang, Hailong Sun, and Philip S Yu. Harnessing multiple large language models: A survey on llm ensemble. *arXiv preprint arXiv:2502.18036*, 2025.
- [7] Isaac Ong, Amjad Almahairi, Vincent Wu, Wei-Lin Chiang, Tianhao Wu, Joseph E Gonzalez, M Waleed Kadous, and Ion Stoica. Routellm: Learning to route llms from preference data. In *The Thirteenth International Conference on Learning Representations*, 2024.
- [8] Shuhao Chen, Weisen Jiang, Baijiong Lin, James Kwok, and Yu Zhang. Routerdc: Query-based router by dual contrastive learning for assembling large language models. *Advances in Neural Information Processing Systems*, 37:66305–66328, 2024.
- [9] Keming Lu, Hongyi Yuan, Runji Lin, Junyang Lin, Zheng Yuan, Chang Zhou, and Jingren Zhou. Routing to the expert: Efficient reward-guided ensemble of large language models. *arXiv preprint arXiv:2311.08692*, 2023.
- [10] Dimitris Stripelis, Zijian Hu, Jipeng Zhang, Zhaozhuo Xu, Alay Diliphai Shah, Han Jin, Yuhang Yao, Salman Avestimehr, and Chaoyang He. Tensoropera router: A multi-model router for efficient llm inference. *arXiv preprint arXiv:2408.12320*, 2024.
- [11] Dujian Ding, Ankur Mallick, Chi Wang, Robert Sim, Subhabrata Mukherjee, Victor Ruhle, Laks VS Lakshmanan, and Ahmed Hassan Awadallah. Hybrid llm: Cost-efficient and quality-aware query routing. *arXiv preprint arXiv:2404.14618*, 2024.
- [12] Tao Feng, Yanzhen Shen, and Jiaxuan You. Graphrouter: A graph-based router for llm selections. *arXiv preprint arXiv:2410.03834*, 2024.
- [13] Quang H Nguyen, Duy C Hoang, Juliette Decugis, Saurav Manchanda, Nitesh V Chawla, and Khoa D Doan. Metallm: A high-performant and cost-efficient dynamic framework for wrapping llms. *arXiv preprint arXiv:2407.10834*, 2024.
- [14] Yang Li. Llm bandit: Cost-efficient llm generation via preference-conditioned dynamic routing. *arXiv preprint arXiv:2502.02743*, 2025.
- [15] Dongfu Jiang, Xiang Ren, and Bill Yuchen Lin. Llm-blender: Ensembling large language models with pairwise ranking and generative fusion. *arXiv preprint arXiv:2306.02561*, 2023.
- [16] Xiaoding Lu, Zongyi Liu, Adian Liusie, Vyas Raina, Vineet Mudupalli, Yuwen Zhang, and William Beauchamp. Blending is all you need: Cheaper, better alternative to trillion-parameters llm. *arXiv preprint arXiv:2401.02994*, 2024.

[17] Hongyi Wang, Felipe Maia Polo, Yuekai Sun, Souvik Kundu, Eric Xing, and Mikhail Yurochkin. Fusing models with complementary expertise. *arXiv preprint arXiv:2310.01542*, 2023.

[18] Lingjiao Chen, Matei Zaharia, and James Zou. Frugalgpt: How to use large language models while reducing cost and improving performance. *arXiv preprint arXiv:2305.05176*, 2023.

[19] Pranjal Aggarwal, Aman Madaan, Ankit Anand, Srividya Pranavi Potharaju, Swaroop Mishra, Pei Zhou, Aditya Gupta, Dheeraj Rajagopal, Karthik Kappagantu, Yiming Yang, et al. Automix: Automatically mixing language models. *Advances in Neural Information Processing Systems*, 37:131000–131034, 2024.

[20] Guillem Ramírez, Alexandra Birch, and Ivan Titov. Optimising calls to large language models with uncertainty-based two-tier selection. *arXiv preprint arXiv:2405.02134*, 2024.

[21] Tal Shnitzer, Anthony Ou, Mírian Silva, Kate Soule, Yuekai Sun, Justin Solomon, Neil Thompson, and Mikhail Yurochkin. Large language model routing with benchmark datasets. *arXiv preprint arXiv:2309.15789*, 2023.

[22] Surya Narayanan Hari and Matt Thomson. Tryage: Real-time, intelligent routing of user prompts to large language models. *arXiv preprint arXiv:2308.11601*, 2023.

[23] Marija Šakota, Maxime Peyrard, and Robert West. Fly-swat or cannon? cost-effective language model choice via meta-modeling. In *Proceedings of the 17th ACM International Conference on Web Search and Data Mining*, pages 606–615, 2024.

[24] Zesen Zhao, Shuowei Jin, and Z Morley Mao. Eagle: Efficient training-free router for multi-llm inference. *arXiv preprint arXiv:2409.15518*, 2024.

[25] Alireza Mohammadshahi, Arshad Rafiq Shaikh, and Majid Yazdani. Routoo: Learning to route to large language models effectively. *arXiv preprint arXiv:2401.13979*, 2024.

[26] Qitian Jason Hu, Jacob Bieker, Xiuyu Li, Nan Jiang, Benjamin Keigwin, Gaurav Ranganath, Kurt Keutzer, and Shriyash Kaustubh Upadhyay. Routerbench: A benchmark for multi-llm routing system. *arXiv preprint arXiv:2403.12031*, 2024.

[27] Yann Dubois, Balázs Galambosi, Percy Liang, and Tatsunori B Hashimoto. Length-controlled alpacaeval: A simple way to debias automatic evaluators. *arXiv preprint arXiv:2404.04475*, 2024.

[28] Clémentine Fourrier, Nathan Habib, Alina Lozovskaya, Konrad Szafer, and Thomas Wolf. Open llm leaderboard v2. [https://huggingface.co/spaces/open-llm-leaderboard/open\\_llm\\_leaderboard](https://huggingface.co/spaces/open-llm-leaderboard/open_llm_leaderboard), 2024.

[29] Percy Liang, Rishi Bommasani, Tony Lee, Dimitris Tsipras, Dilara Soylu, Michihiro Yasunaga, Yian Zhang, Deepak Narayanan, Yuhuai Wu, Ananya Kumar, et al. Holistic evaluation of language models. *arXiv preprint arXiv:2211.09110*, 2022.

[30] Tony Lee, Haoqin Tu, Chi Heem Wong, Wenhao Zheng, Yiyang Zhou, Yifan Mai, Josselin Roberts, Michihiro Yasunaga, Huaxiu Yao, Cihang Xie, et al. Vhelm: A holistic evaluation of vision language models. *Advances in Neural Information Processing Systems*, 37:140632–140666, 2024.

[31] Jacob Devlin, Ming-Wei Chang, Kenton Lee, and Kristina Toutanova. Bert: Pre-training of deep bidirectional transformers for language understanding. In *Proceedings of the 2019 conference of the North American chapter of the association for computational linguistics: human language technologies, volume 1 (long and short papers)*, pages 4171–4186, 2019.

[32] Ziyang Jiang, Rui Meng, Xinyi Yang, Semih Yavuz, Yingbo Zhou, and Wenhui Chen. Vlm2vec: Training vision-language models for massive multimodal embedding tasks. *arXiv preprint arXiv:2410.05160*, 2024.

[33] Yaniv Leviathan, Matan Kalman, and Yossi Matias. Fast inference from transformers via speculative decoding. In *International Conference on Machine Learning*, pages 19274–19286. PMLR, 2023.

- [34] Kazuki Egashira, Mark Vero, Robin Staab, Jingxuan He, and Martin Vechev. Exploiting llm quantization. *arXiv preprint arXiv:2405.18137*, 2024.
- [35] Xiaoyuan Su and Taghi M Khoshgoftaar. A survey of collaborative filtering techniques. *Advances in artificial intelligence*, 2009(1):421425, 2009.
- [36] Badrul Sarwar, George Karypis, Joseph Konstan, and John Riedl. Item-based collaborative filtering recommendation algorithms. In *Proceedings of the 10th international conference on World Wide Web*, pages 285–295, 2001.
- [37] Arnaud De Myttenaere, Bénédicte Le Grand, Boris Golden, and Fabrice Rossi. Reducing offline evaluation bias in recommendation systems. *arXiv preprint arXiv:1407.0822*, 2014.
- [38] Shafiq Rayhan Joty Caiming Xiong Yingbo Zhou Semih Yavuz Rui Meng, Ye Liu. Sfr-embedding-mistral:enhance text retrieval with transfer learning. Salesforce AI Research Blog, 2024.
- [39] Andrei Nikolaevich Kolmogorov and Vladimir Mikhailovich Tikhomirov.  $\varepsilon$ -entropy and  $\varepsilon$ -capacity of sets in function spaces. *Uspekhi Matematicheskikh Nauk*, 14(2):3–86, 1959.
- [40] Ulrike von Luxburg and Olivier Bousquet. Distance-based classification with lipschitz functions. *Journal of Machine Learning Research*, 5(Jun):669–695, 2004.
- [41] Andrew R Barron. Universal approximation bounds for superpositions of a sigmoidal function. *IEEE Transactions on Information theory*, 39(3):930–945, 1993.
- [42] Dmitry Yarotsky. Error bounds for approximations with deep relu networks. *Neural networks*, 94:103–114, 2017.
- [43] Peter L Bartlett, Dylan J Foster, and Matus J Telgarsky. Spectrally-normalized margin bounds for neural networks. *Advances in neural information processing systems*, 30, 2017.
- [44] Noah Golowich, Alexander Rakhlin, and Ohad Shamir. Size-independent sample complexity of neural networks. In *Conference On Learning Theory*, pages 297–299. PMLR, 2018.

## A Additional Related Works

Beyond the core routing approaches discussed in Section 2, several other research directions are relevant to our investigation of LLM routing mechanisms.

**LLM Inference Optimization** Routing can be viewed as one component of the broader challenge of optimizing LLM inference. Complementary approaches include speculative decoding [33], quantization [34], and hardware-specific optimizations. Our work on efficient routing complements these techniques, as the benefits of selecting the most appropriate model can be combined with optimizations to the inference process itself.

**Connections to Recommendation Systems** LLM routing shares fundamental similarities with recommendation systems, where the goal is to match users (queries) with items (models) that maximize utility. Several techniques from recommender systems research have direct analogs in routing approaches. Matrix factorization methods like those used in RouteLLM [7] mirror collaborative filtering techniques in recommendation [35]. Similarly, our kNN approach resembles item-based neighborhood methods that recommend items based on similarity to previously rated items [36]. Content-based recommendation techniques that leverage item features parallel our embedding-based routing approaches. Even the dual optimization of performance and cost in routing mirrors multi-objective recommendation systems that balance relevance with diversity or novelty [37]. This connection offers promising opportunities to adapt proven recommendation techniques to the routing domain, particularly for handling cold-start problems with new queries or models, and for developing effective hybrid routing strategies.

## B Routing Benchmarks

In this section, we provide detailed information about our benchmark construction methodology, model selection criteria, and evaluation protocols for both text and vision-language routing benchmarks.

### B.1 Text-Based Routing Benchmarks

We construct comprehensive benchmarks based on three established LLM evaluation frameworks: AlpacaEval, Open LLM Leaderboard v2, and HELM-Lite, as well as incorporating RouterBench. Our goal is to provide a diverse set of routing scenarios that reflect real-world deployment challenges.

**Model Selection** For each benchmark, we select three model families with multiple variants per family to represent realistic routing scenarios:

- **AlpacaEval:** We include OpenAI models, Claude models, and Mistral models.
- **Open LLM Leaderboard:** We include LLaMA3 variants, Qwen2.5 variants, and Yi-1.5 variants.
- **HELM-Lite:** We include OpenAI models, Claude models, and Google Gemini models.
- **RouterBench:** We use all 11 models provided in the original benchmark.

Please refer to Table B.1 for the list of models and their costs.

**Task Coverage** Our benchmarks span a wide range of task categories:

- **AlpacaEval:** Instruction following tasks evaluated through human preference alignment.
- **Open LLM Leaderboard:** Mathematical reasoning, knowledge-based reasoning and instruction following tasks.
- **HELM-Lite:** Knowledge-intensive tasks, reasoning tasks, and instruction following capabilities.
- **RouterBench:** Six tasks spanning mathematical reasoning, code generation, knowledge, and commonsense reasoning.

**Performance Scoring Methodology** For each benchmark, we use evaluation metrics aligned with their respective leaderboards:

- **AlpacaEval:** We use length-controlled win rates against the reference model.
- **Open LLM Leaderboard:** We use accuracy metrics for each task as reported in the leaderboard.
- **HELM-Lite:** We use the benchmark-specific metrics as reported in the leaderboard.
- **RouterBench:** We use the performance scores provided in the original benchmark.

**Cost Calculation** We calculate costs based on actual pricing of each API, using:

$$c(x, m) = \text{InputTokens} \times \text{InputPrice}_m + \text{OutputTokens} \times \text{OutputPrice}_m$$

For open-source models, we estimate costs using the pricing of equivalent commercial offerings from TogetherAI.

## B.2 Vision-Language Routing Benchmarks

To address the growing importance of multi-modal systems, we develop the first benchmark for routing between vision-language models. This benchmark assesses how routing methods perform when inputs span different modalities. We utilize the existing evaluation outcomes from vHELM leaderboard.

**Model Selection** We focus on two leading vision-language model families - OpenAI models and Claude models - with multiple variants representing different capability-cost tradeoffs. Table B.2 list the candidate models and their costs.

**Dataset Selection** We select five diverse vision-language datasets with varying task complexity:

- **Blink:** Tests basic visual perception and object recognition capabilities.
- **Flickr30k:** Evaluates natural image description and scene understanding.
- **MathVista:** Challenges models with mathematical reasoning over visual inputs.
- **MME:** A comprehensive evaluation benchmark covering multiple vision-language capabilities.
- **MMMU:** Tests multi-modal understanding across challenging academic domains.

Each dataset presents unique routing challenges, as models show different strengths across visual understanding tasks. For example, some models excel at detailed image description but struggle with visual reasoning tasks.

## B.3 Evaluation Protocol

### B.3.1 AUC Score Calculation Methodology

To evaluate utility prediction approaches, we calculate the area under the curve (AUC) of the non-decreasing convex hull in the cost-performance space using the following procedure:

1. For a given query  $x$ , we obtain predicted utility scores  $\hat{u}(x, m) = \hat{s}(x, m) - \lambda \times \hat{c}(x, m)$  for each model  $m \in \mathcal{M}$  across various values of  $\lambda$ .
2. For each  $\lambda$  value, we select the model with the highest predicted utility:  $m_\lambda = \arg \max_{m \in \mathcal{M}} \hat{u}(x, m)$ .
3. We plot the actual performance-cost pairs  $(c(x, m_\lambda), s(x, m_\lambda))$  in the cost-performance space.
4. We compute the non-decreasing convex hull of these points to obtain the Pareto-optimal frontier.
5. The AUC is calculated as the area under this frontier, normalized so that the maximum score is 100 and the maximum cost is 1.

This approach ensures that routers are evaluated on their ability to make optimal trade-offs across the entire spectrum of cost-performance preferences.

## B.4 Data Splits and Reproducibility

To ensure reproducible evaluation, we use the following data splits:

- For all benchmarks, we create random splits over prompts with 70% training, 10% validation, and 20% test data.
- For support set experiments, we ensure no leakage between support sets and test queries.
- All random seeds are fixed and documented in our code to ensure reproducibility.

Our benchmark construction methodology ensures comprehensive evaluation across diverse tasks, models, and modalities, providing a robust foundation for comparing different routing approaches.

## C Routing Approaches

This section provides detailed implementation information for all routing approaches evaluated in our study, including architecture specifications, hyperparameter settings, training procedures, and computational requirements.

### C.1 Input Representations

For all routing approaches, we use consistent input representations to ensure fair comparison:

**Text Embeddings** For text-only queries, we primarily use BERT [31] base model (768-dimensional embeddings) to encode input queries. We take the [CLS] token embedding as the query representation. In our ablation studies (Table 6), we also experiment with SFR [38] embeddings (4096-dimensional) to assess the impact of embedding quality on routing performance. All embeddings are L2-normalized to unit length.

**Vision-Language Embeddings** For multi-modal queries, we employ VLM2Vec [32] to extract unified representations of image-text pairs. Specifically, we utilize the Qwen7B-based variant, which generates 3584-dimensional embeddings that effectively capture both textual content and visual features in a shared embedding space.

### C.2 Routing Model Architectures

**kNN Router** Our kNN implementation uses cosine similarity to identify the nearest neighbors in the embedding space. For utility prediction, we compute the weighted average of performance scores and costs from the  $k$  nearest neighbors:

$$\hat{s}(x, m) = \frac{1}{k} \sum_{i=1}^k s(x_i, m), \quad \hat{c}(x, m) = \frac{1}{k} \sum_{i=1}^k c(x_i, m)$$

For model selection, we use the majority voting mechanism, where each neighbor votes for the model that maximizes its utility score.

**Linear Router** For utility prediction, we implement a linear regression model that maps query embeddings directly to performance scores and costs:

$$\hat{s}(x, m) = W_s^m \cdot \text{emb}(x) + b_s^m, \quad \hat{c}(x, m) = W_c^m \cdot \text{emb}(x) + b_c^m \quad (\text{C.1})$$

where  $W_s^m, W_c^m \in \mathbb{R}^{768}$  and  $b_s^m, b_c^m \in \mathbb{R}$  are learnable parameters for each model  $m$ . For model selection, we use a multi-class logistic regression:

$$p(m|x) = \text{softmax}(W \cdot \text{emb}(x) + b)$$

where  $W \in \mathbb{R}^{M \times 768}$  and  $b \in \mathbb{R}^M$  are learnable parameters.

**Linear Matrix Factorization (MF) Router** This approach assigns a learnable embedding to each model and predicts performance through the interaction between query and model embeddings:

$$\hat{s}(x, m) = \text{emb}(x)^\top \cdot W_s \cdot \text{emb}(m) + b_s, \quad \hat{c}(x, m) = \text{emb}(x)^\top \cdot W_c \cdot \text{emb}(m) + b_c$$

where  $W_s, W_c \in \mathbb{R}^{768 \times d_m}$ ,  $\text{emb}(m) \in \mathbb{R}^{d_m}$  is the learnable embedding for model  $m$  (we use  $d_m = 128$ ), and  $b_s, b_c \in \mathbb{R}$  are learnable biases.

**MLP Router** Our MLP consists of 3 fully-connected layers with ReLU activations:

$$\hat{s}(x, m) = \text{MLP}_s^m(\text{emb}(x)), \quad \hat{c}(x, m) = \text{MLP}_c^m(\text{emb}(x))$$

The architecture uses 100 dimensions for each hidden layer.

**MLP Matrix Factorization (MF) Router** Similar to Linear MF, but replaces the linear projection with an MLP:

$$\hat{s}(x, m) = \text{MLP}_s([\text{emb}(x); \text{emb}(m)]), \quad \hat{c}(x, m) = \text{MLP}_c([\text{emb}(x); \text{emb}(m)])$$

where  $[;]$  denotes concatenation. The MLP has architecture use 100 hidden units with ReLU activations.

**Graph Router** We implement a bipartite graph neural network where queries and models form nodes. Each query-model pair is connected by directed edges containing features that represent scores, token counts, and neighborhood information. Our implementation uses the GeneralConv class from PyTorch Geometric with the following architecture:

$$\begin{aligned} h_x^{(0)} &= W_{\text{proj}} \cdot \text{emb}(x), \quad h_m^{(0)} = \text{emb}(m) \\ e_{xm}^{(0)} &= W_{\text{edge}} \cdot [s_{xm}, t_{xm}, \text{mask}_{xm}] \\ h_i^{(l+1)} &= \sigma \left( \text{BN}^{(l)} \left( \text{GNN}^{(l)} \left( h_i^{(l)}, h_j^{(l)} \mid j \in \mathcal{N}(i), e_{ij}^{(l)} \right) \right) \right) \end{aligned}$$

where  $\text{emb}(m)$  is a learned embedding for each model,  $s_{xm}$  and  $t_{xm}$  are the score and token count features between query  $x$  and model  $m$ ,  $\text{mask}_{xm}$  indicates whether the edge features are observed or missing, BN is batch normalization, and  $\sigma$  is ReLU. The graph is enriched with  $k$ -nearest neighbor information from a pre-computed benchmark dataset. After message passing through multiple GNN layers (we use 2 layers with hidden dimension 128), the final prediction is computed using an MLP over the concatenated node representations of each query-model pair.

**Attentive Router** This approach employs a Conditional Neural Process architecture with both self-attention and cross-attention mechanisms to process nearest neighbor examples:

$$\begin{aligned} \text{support} &= (x_i, s(x_i, m), c(x_i, m)) \mid x_i \in \text{kNN}(x, k) \\ Z &= \text{SelfAttention}(\text{support}) \\ \text{latent}(x, m) &= \text{CrossAttention}(Q = \text{emb}(x), K = \text{emb}(\text{support}), V = Z) \\ \hat{s}(x, m) &= \text{MLP}_s(\text{latent}(x, m)), \quad \hat{c}(x, m) = \text{MLP}_c(\text{latent}(x, m)), \end{aligned}$$

where the self-attention module applies permutation-invariant processing to the support set, and the cross-attention module allows the query to attend to the processed support set. For each model, we retrieve  $k$ -nearest neighbors with their corresponding scores and token counts, and project them to a shared embedding space. The architecture uses multi-head attention (4 heads with dimension 32 per head), followed by MLP prediction heads for both score and token count estimation.

**Double Attentive Router** Extends the Attentive Router by processing the support set with a dual attention mechanism that captures both query-level and model-level interactions:

$$\begin{aligned} \text{support} &= (x_i, s(x_i, m), c(x_i, m)) \mid x_i \in \text{kNN}(x, k), m \in \mathcal{M} \\ Z &= \text{DoubleAttention}(\text{support}) \\ \text{latent}(x, m) &= \text{CrossAttention}(Q = \text{emb}(x), K = \text{emb}(\text{support}), V = Z) \\ \hat{s}(x, m) &= \text{MLP}_s(\text{latent}(x, m)), \quad \hat{c}(x, m) = \text{MLP}_c(\text{latent}(x, m)) \end{aligned}$$

where the double attention mechanism applies attention operations across both examples and models, allowing for richer representations that capture cross-model dependencies. The support set is organized as a 3D tensor (batch  $\times$  models  $\times$  examples) and processed with sequential attention operations. This architecture enables the router to model complex interactions between different models on similar queries, thereby improving routing accuracy across the model pool.

### C.3 Training Protocols

**Loss Functions** For utility prediction models, we use mean squared error (MSE) loss for both score and cost prediction:

$$\mathcal{L} = \text{MSE}(\hat{s}(x, m), s(x, m)) + \alpha \cdot \text{MSE}(\hat{c}(x, m), c(x, m))$$

where  $\alpha$  is a weighting coefficient that balances performance and cost prediction.

For model selection approaches, we use cross-entropy loss:

$$\mathcal{L} = - \sum_{m \in \mathcal{M}} y_m \log(p(m|x))$$

where  $y_m = 1$  if  $m$  is the optimal model for query  $x$  under the specified trade-off parameter  $\lambda$ , and 0 otherwise.

## D Additional Results

In the main text, we report RouterBench results as averages across all six datasets. For a more granular analysis, Tables D.1 and D.2 provide the detailed performance breakdown for each individual dataset under the utility prediction and model selection formulations, respectively. Additionally, Tables D.3 and D.4 present detailed results across three different preference settings for the text-based and multi-modal (VLM) routing benchmarks.

For model selection approaches, there is no straightforward way to obtain the entire cost-quality Pareto front. Instead, we evaluate these routers using three distinct preference settings and report the final utility scores, following standard evaluation protocols in the literature. However, we must emphasize that reported utility scores alone can sometimes present an incomplete picture. The utility function combines both performance and cost in a weighted sum  $(s(x, m) - \lambda \cdot c(x, m))$ , but this single metric obscures the actual trade-off between these two dimensions. For instance, two routing approaches might achieve similar utility scores through different means—one by selecting higher-performing but costlier models, and another by choosing more cost-efficient models with slightly lower performance. Without visualizing the actual cost-performance points, it becomes difficult to understand these different strategies and their practical implications for deployment scenarios where budget constraints or performance requirements might vary.

To provide a more complete picture of this trade-off, we plot the actual cost-performance relationships in Fig.D.1 and Fig.D.2 for text-based and vision-language model routing benchmarks, respectively. These visualizations reveal the direct relationship between model cost and performance without the abstraction of a combined utility metric. The results demonstrate that simple kNN-based approaches remain highly competitive when compared to more complex routing methods operating under the same cost budget. In many cases, kNN routers achieve comparable or better performance than sophisticated neural architectures while maintaining similar cost efficiency, further supporting our core finding that simple, non-parametric routing methods offer a compelling alternative to complex learned approaches.

Notably, these plots often do not demonstrate a monotonic trend across the three preference settings, highlighting a significant limitation of the model selection formulation: the difficulty in precisely controlling the cost budget through preference parameter adjustment alone. This non-monotonic behavior underscores the challenge of balancing performance and cost when routing decisions are made directly, rather than through explicit utility estimation, and further motivates our parallel investigation of utility prediction approaches that allow for more flexible exploration of the entire Pareto front.

## E Proof

**Theorem 1.** *For a query distribution  $\mathcal{D}$  with  $\delta$ -locality in utility space:*

(a) *A kNN router requires a training sample size of  $\Theta\left(\frac{C_{\mathcal{X},d}}{\delta^d} \log\left(\frac{1}{\alpha}\right)\right)$  to achieve expected regret  $O(\epsilon(\delta))$  with probability  $1 - \alpha$ , where  $d$  is the intrinsic dimension of the embedding space and  $C_{\mathcal{X},d}$  is a constant depending on the space.*

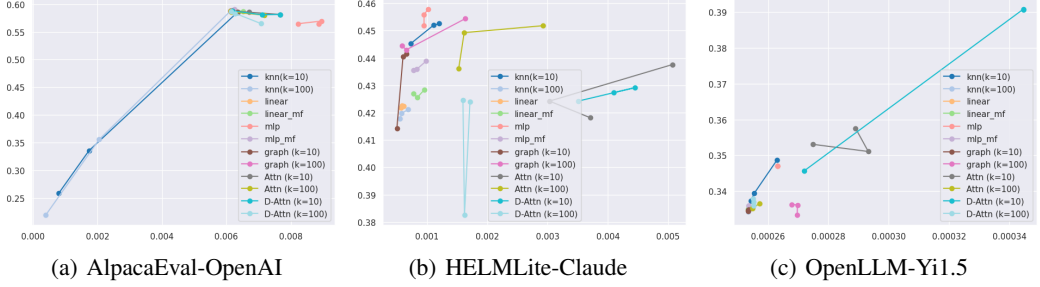


Figure D.1: Cost-Quality tradeoff for text-based routing benchmarks using model selection approaches.

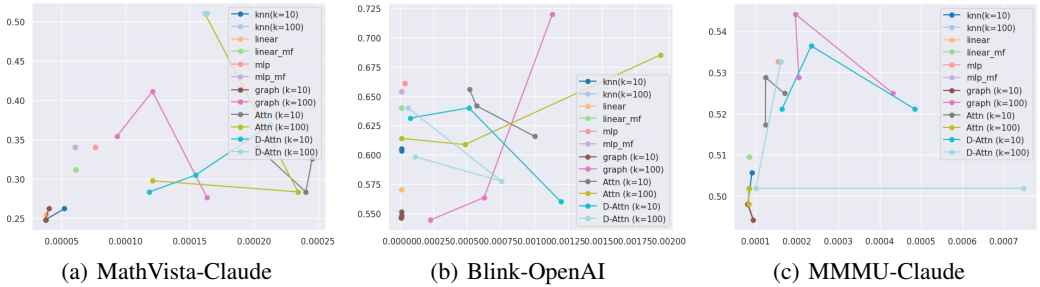


Figure D.2: Cost-Quality tradeoff for VLM routing benchmarks using model selection approaches.

(b) A parametric router with  $L$  Lipschitz-continuous layers requires a training sample size of  $\Omega(L/\epsilon(\delta)^2)$  to achieve the same regret bound.

*Proof.* We first derive the sample complexity for kNN and parametric approaches and then compare them.

### Part 1: kNN Router Sample Complexity

Let  $\mathcal{X}$  be the query embedding space with intrinsic dimension  $d$  and  $u : \mathcal{X} \times \mathcal{M} \rightarrow \mathbb{R}$  be the true utility function mapping query-model pairs to utility scores. By the  $\delta$ -locality property, for any two queries  $x_1, x_2$  with  $d(x_1, x_2) < \delta$ , we have  $|u(x_1, m) - u(x_2, m)| < \epsilon(\delta)$  for all models  $m \in \mathcal{M}$ .

**Step 1:** First, we establish what makes a kNN estimate accurate.

For a query  $x$ , let  $\hat{u}(x, m)$  be the kNN estimate of model  $m$ 's utility:

$$\hat{u}(x, m) = \frac{1}{k} \sum_{x_i \in \mathcal{N}_k(x)} u(x_i, m),$$

where  $\mathcal{N}_k(x)$  is the set of  $k$  nearest neighbors of  $x$  in the training set. By the  $\delta$ -locality property, if all  $k$  neighbors are within distance  $\delta$  of  $x$ , then the approximation error is bounded by  $\epsilon(\delta)$ :

$$|\hat{u}(x, m) - u(x, m)| < \epsilon(\delta).$$

**Step 2:** We analyze the sample complexity needed to ensure sufficient neighborhood coverage.

Let  $N(\mathcal{X}, \delta/2)$  be the  $\delta/2$ -covering number of  $\mathcal{X}$ , which is the minimum number of balls of radius  $\delta/2$  needed to cover  $\mathcal{X}$ . For a space with intrinsic dimension  $d$ , this covering number scales as  $N(\mathcal{X}, \delta/2) = \Theta(C_{\mathcal{X}, d}/\delta^d)$ , where  $C_{\mathcal{X}, d}$  is a constant depending on the properties of  $\mathcal{X}$  [39, 40].

Let's divide the space into  $N(\mathcal{X}, \delta/2)$  regions corresponding to this cover. If we ensure that each region contains at least  $k$  training points, then any query will have at least  $k$  neighbors within distance  $\delta$ .

**Step 3:** We compute the sample size needed to populate each region with enough points.

Assume we draw  $n$  training samples i.i.d. from distribution  $\mathcal{D}$ . For a region  $R_i$  with probability mass  $\mathcal{D}(R_i)$ , the probability that fewer than  $k$  samples fall into  $R_i$  is:

$$P(\text{fewer than } k \text{ samples in } R_i) = \sum_{j=0}^{k-1} \binom{n}{j} \mathcal{D}(R_i)^j (1 - \mathcal{D}(R_i))^{n-j}.$$

We need to ensure that with high probability,  $X_i \geq k$  for all regions.

For a single region  $R_i$ , using the Chernoff bound for the lower tail of a binomial distribution with mean  $\mu = nD(R_i)$ :

$$P(X_i \leq (1-t)\mu) \leq \exp(-t^2\mu/2) \quad \text{for any } 0 < t < 1$$

Setting  $(1-t)nD(R_i) = k$ , which implies  $t = 1 - \frac{k}{nD(R_i)}$ , and imposing the constraint  $nD(R_i) \geq 2k$  (ensuring  $t \geq \frac{1}{2}$ ), we get:

$$P(X_i < k) \leq \exp(-t^2 nD(R_i)/2) \leq \exp\left(-\frac{(1/4)nD(R_i)}{2}\right) = \exp\left(-\frac{nD(R_i)}{8}\right)$$

For the union bound to work across all  $N(X, \delta/2)$  regions, we need:

$$P(X_i < k) \leq \frac{\alpha}{N(X, \delta/2)} \quad \text{for each region } R_i$$

Therefore:

$$\exp\left(-\frac{nD(R_i)}{8}\right) \leq \frac{\alpha}{N(X, \delta/2)}$$

Taking logarithms:

$$\begin{aligned} -\frac{nD(R_i)}{8} &\leq \ln(\alpha) - \ln(N(X, \delta/2)) \\ nD(R_i) &\geq 8 \ln\left(\frac{1}{\alpha}\right) + 8 \ln(N(X, \delta/2)) \end{aligned}$$

To maintain consistency with our constraint  $nD(R_i) \geq 2k$ , we require:

$$\begin{aligned} 2k &\geq 8 \ln\left(\frac{1}{\alpha}\right) + 8 \ln(N(X, \delta/2)) \\ k &\geq 4 \ln\left(\frac{1}{\alpha}\right) + 4 \ln(N(X, \delta/2)) \end{aligned}$$

To satisfy  $nD(R_i) \geq 2k$  for all regions, we need:

$$n \geq \frac{2k}{\min_i D(R_i)}$$

Under a reasonable assumption that the distribution  $\mathcal{D}$  doesn't assign extremely small probability to any significant region (specifically,  $\min_i D(R_i) \geq \frac{c}{N(X, \delta/2)}$  for some constant  $c > 0$ ), we get:

$$n \geq \frac{2kN(X, \delta/2)}{c} = \Theta\left(\frac{k \cdot C_{X,d}}{c \cdot \delta^d}\right)$$

Substituting  $k = \Theta\left(\ln\left(\frac{1}{\alpha}\right) + \ln(N(X, \delta/2))\right) = \Theta\left(\ln\left(\frac{1}{\alpha}\right) + \ln\left(\frac{C_{X,d}}{\delta^d}\right)\right)$ :

$$\begin{aligned} n &= \Theta\left(\frac{C_{X,d}}{\delta^d} \cdot \ln\left(\frac{1}{\alpha}\right) + \frac{C_{X,d}}{\delta^d} \cdot \ln\left(\frac{C_{X,d}}{\delta^d}\right)\right) \\ n &= \Theta\left(\frac{C_{X,d}}{\delta^d} \cdot \ln\left(\frac{1}{\alpha}\right) + \frac{C_{X,d}}{\delta^d} \cdot \left(\ln(C_{X,d}) + d \cdot \ln\left(\frac{1}{\delta}\right)\right)\right) \end{aligned}$$

$$n = \Theta \left( \frac{C_{X,d}}{\delta^d} \cdot \ln \left( \frac{1}{\alpha} \right) + \frac{C_{X,d} \cdot d}{\delta^d} \cdot \ln \left( \frac{1}{\delta} \right) \right)$$

For fixed  $\delta$  and decreasing  $\alpha$ , the dominant term is  $\Theta \left( \frac{C_{X,d}}{\delta^d} \cdot \ln \left( \frac{1}{\alpha} \right) \right)$ .

By the union bound, the probability that any region has fewer than  $k$  samples is at most  $\alpha$ . This ensures that with probability at least  $1 - \alpha$ , every query point has at least  $k$  neighbors within distance  $\delta$ .

**Step 4:** We connect this to the regret bound.

With probability at least  $1 - \alpha$ , every query has at least  $k$  neighbors within distance  $\delta$ . For such queries, by the  $\delta$ -locality property, the kNN router achieves regret  $O(\epsilon(\delta))$  since:  $|\hat{u}(x, m) - u(x, m)| < \epsilon(\delta)$  for all models  $m$ .

When selecting the model with the highest predicted score:

$$m_{kNN} = \arg \max_m \hat{u}(x, m),$$

we have:  $u(x, m_{kNN}) > \hat{u}(x, m_{kNN}) - \epsilon(\delta) \leq \hat{u}(x, m*) - \epsilon(\delta) > u(x, m*) - 2\epsilon(\delta)$ .

Therefore, the regret is bounded by:

$$u(x, m*) - u(x, m_{kNN}) < 2\epsilon(\delta)$$

**Part 2: Parametric Router Sample Complexity** For a parametric router with  $L$  Lipschitz-continuous layers, we analyze the sample complexity required to learn an accurate model of the performance function.

**Step 1:** We establish the approximation capacity.

Following the results of [41] and [42], a neural network with  $L$  layers and width  $W$  can approximate functions in certain smoothness classes to accuracy  $\epsilon$  if  $W = \Omega((1/\epsilon)^{d/L})$ , where  $d$  is the input dimension.

For the utility function  $u(x, m)$ , which maps from  $\mathbb{R}^d \times \mathcal{M}$  to  $\mathbb{R}$ , a network with  $L$  Lipschitz-continuous layers requires  $\Omega(L \cdot (1/\epsilon)^{d/L})$  parameters to achieve uniform approximation error at most  $\epsilon$ .

**Step 2:** We relate approximation capacity to sample complexity.

By standard generalization bounds for neural networks [43, 44], the sample complexity to learn the parameters of such a network with generalization error at most  $\epsilon$  is:

$$n_{\text{param}} = \Omega \left( \frac{W \cdot L \cdot \log(W)}{\epsilon^2} \right)$$

Substituting  $W = \Omega(L \cdot (1/\epsilon)^{d/L})$ , we get:

$$n_{\text{param}} = \Omega \left( \frac{L^2 \cdot (1/\epsilon)^{d/L} \cdot \log(L \cdot (1/\epsilon)^{d/L})}{\epsilon^2} \right)$$

For small values of  $\epsilon$  and moderate values of  $L$ , the dominant term is  $\Omega(L/\epsilon^2)$ , which represents a lower bound on the sample complexity.

**Step 3:** We connect to the regret bound.

To achieve a regret bound of  $O(\epsilon(\delta))$ , the parametric model must approximate the true performance function with error at most  $\epsilon(\delta)/2$  uniformly over the query space. This requires a sample complexity of  $\Omega(L/\epsilon(\delta)^2)$ .

**Part 3: Comparison** Now we compare the sample complexity of the two approaches:

$$\text{kNN router: } \Theta \left( \frac{C_{X,d}}{\delta^d} \cdot \log \left( \frac{1}{\alpha} \right) \right)$$

Parametric router:  $\Omega(L/\epsilon(\delta)^2)$

For small values of  $\epsilon(\delta)$  (high accuracy requirements), the parametric router's sample complexity grows quadratically with  $1/\epsilon(\delta)$ , while the kNN router's complexity depends on  $1/\delta^d$  and only logarithmically on  $1/\alpha$ .

When the embedding space has a low intrinsic dimension  $d$  (which is often the case for well-designed embedding spaces), and  $\epsilon(\delta)$  decreases rapidly with  $\delta$  (strong locality property), the kNN router requires significantly fewer training samples than a parametric router to achieve the same regret bound.

□

Table B.1: Candidate models and their costs for text-based routing benchmark.

Benchmark	Model Family	Candidate Models	Input cost (\$ per 1M tokens)	Output cost (\$ per 1M tokens)
ALpacaEval	OpenAI Family	gpt-3.5-turbo-0301	1.5	2.0
		gpt-3.5-turbo-0613	1.5	2.0
		gpt-3.5-turbo-1106	1.0	2.0
		gpt-4-0125-preview	10	30
		gpt-4o-2024-05-13	5	15
		gpt-4	30	60
		gpt-4-0314	30	60
		gpt-4-0613	30	60
	Claude Family	gpt-4-1106-preview	10	30
		claude-2	8	24
	Mistral Family	claude-2.1	8	24
		claude-3-5-sonnet-20240620	3	15
		claude-3-opus-20240229	15	75
		claude-3-sonnet-20240229	3	15
		claude-instant-1.2	0.8	2.4
		Mistral-7B-Instruct-v0.2	0.25	0.25
Open LLM Leaderboard v2	Qwen2.5	Mixtral-8x22B-Instruct-v0.1	2	6
		Mixtral-8x7B-Instruct-v0.1	0.7	0.7
		mistral-large-2402	8	24
		mistral-medium	2.7	8.1
		Qwen2.5-0.5B-Instruct	0.08	0.08
		Qwen2.5-1.5B-Instruct	0.2	0.2
	Llama3	Qwen2.5-7B-Instruct	0.3	0.3
		Qwen2.5-14B-Instruct	0.8	0.8
	Yi1.5	Qwen2.5-32B-Instruct	0.8	0.8
		Qwen2.5-72B-Instruct	1.2	1.2
	Llama3	Llama-3-8B-Instruct	0.2	0.2
		Llama-3-70B-Instruct	0.9	0.9
	Yi1.5	Yi-1.5-6B-Chat	0.3	0.3
		Yi-1.5-9B-Chat	0.4	0.4
		Yi-1.5-34B-Chat	0.8	0.8
HLM-Lite	OpenAI Family	gpt-4o-2024-05-13	5.0	15.0
		gpt-4o-mini-2024-07-18	0.15	0.6
		gpt-3.5-turbo-0613	1.5	2.0
		gpt-4-0613	30	60
		gpt-4-turbo-2024-04-09	10	30
		gpt-4-1106-preview	10	30
	Claude Family	claude-3-5-sonnet-20240620	3	15
		claude-3-opus-20240229	15	75
		claude-3-sonnet-20240229	3	15
		claude-3-haiku-20240307	0.25	1.25
		claude-2	8	24
		claude-instant-v1	0.8	2.4
	Google Family	claude-v1.3	8	24
		claude-2.1	8	24
		claude-instant-1.2	0.8	2.4
		gemini-1.0-pro-002	0.5	1.5
		gemini-1.0-pro-001	0.5	1.5
		gemini-1.5-pro-001	3.5	10.5
RouterBench	RouterBench	gemini-1.5-flash-001	0.075	0.3
		text-bison-001	0.5	1.5
		text-unicorn-001	7.0	21.0
		gemma-2-9b-it	0.2	0.2
		gemma-2-27b-it	0.6	0.6
		gemma-7b	0.1	0.1
		gpt-3.5	1.0	2.0
		claude-instant-v1	0.8	2.4
		claude-v1	8.0	24.0
		claude-v2	8.0	24.0

Table B.2: Candidate models and their costs for VLM routing benchmark.

Benchmark	Model Family	Candidate models	Input cost (\$ per 1M tokens)	Output cost (\$ per 1M tokens)
vHLM	OpenAI Family	gpt-4-turbo-2024-04-09	10	30
		gpt-4.1-2025-04-14	2	8
		gpt-4.1-mini-2025-04-14	0.4	1.6
		gpt-4.1-nano-2025-04-14	0.1	0.4
		gpt-4.5-preview-2025-02-27	75	150
		gpt-4o-2024-05-13	5	15
		gpt-4o-2024-08-06	2.5	10
		gpt-4o-2024-11-20	2.5	10
		gpt-4o-mini-2024-07-18	0.15	0.6
		o1-2024-12-17	15	60
		o3-2025-04-16	10	40
		o4-mini-2025-04-16	1.1	4.4
	Claude Family	claude-3-5-sonnet-20240620	3	15
		claude-3-5-sonnet-20241022	3	15
		claude-3-7-sonnet-20250219	3	15
		claude-3-7-sonnet-20250219-thinking-64k	3	15
		claude-3-haiku-20240307	0.8	4
		claude-3-opus-20240229	15	75
		claude-3-sonnet-20240229	3	15

Table D.1: AUC score on RouterBench using utility prediction routing. Higher is better.

	Arcc	GSM	MBPP	MMLU	Hellaswag	Winogrande	Avg
Oracle	97.99	74.59	85.02	96.44	97.92	99.48	91.91
Random	64.67	52.47	50.74	57.41	54.74	49.55	54.93
kNN (k=10)	88.15	63.82	60.16	73.91	87.93	71.35	74.22
kNN (k=100)	91.80	64.72	58.67	80.81	89.39	77.91	77.22
Linear	92.27	65.50	60.76	81.05	87.87	78.63	77.68
Linear (MF)	91.80	64.55	60.08	80.91	88.07	78.18	77.27
MLP	91.78	65.03	59.35	80.22	87.85	78.22	77.08
MLP (MF)	91.70	65.38	60.05	80.94	87.85	78.50	77.40
Graph (k=10)	91.70	62.23	56.36	80.76	87.89	78.52	76.24
Graph (k=100)	91.39	62.76	59.38	80.88	87.89	78.93	76.87
Attn (k=10)	89.49	62.08	56.36	72.12	87.88	73.26	73.53
Attn (k=100)	91.63	64.07	60.85	81.01	87.86	78.82	77.37
D-Attn (k=10)	89.43	62.51	58.67	74.15	87.91	73.72	74.40
D-Attn (k=100)	91.67	64.48	60.14	80.71	89.40	78.46	77.48

Table D.2: Utility score on RouterBench using selection based routing. Higher is better.

		Arcc	GSM	MBPP	MMLU	Hellaswag	Winogrande	Avg
High-Performance	kNN (k=10)	64.75	50.30	36.41	55.31	59.74	51.95	53.08
	kNN (k=100)	64.53	50.89	33.32	53.39	59.74	52.49	52.39
	Linear	64.53	50.86	33.32	53.39	59.74	52.49	52.39
	Linear (MF)	64.53	50.88	33.32	53.39	59.74	52.49	52.39
	MLP	64.53	51.40	42.60	53.39	59.74	52.47	54.02
	MLP (MF)	64.53	50.86	33.32	53.39	59.74	52.49	52.39
	Graph (k=10)	64.53	50.90	32.54	53.39	59.74	53.27	52.40
	Graph (k=100)	65.95	50.90	31.73	54.76	59.74	57.21	53.38
	Attn (k=10)	67.32	50.64	37.85	56.49	59.74	54.03	54.35
	Attn (k=100)	64.35	51.18	41.57	55.80	59.74	36.20	51.47
	D-Attn (k=10)	66.35	44.22	35.53	46.06	59.74	50.64	50.42
	D-Attn (k=100)	65.13	51.05	32.51	54.77	25.57	54.02	47.18
	kNN (k=10)	64.53	50.23	36.31	55.06	59.74	52.49	53.06
	kNN (k=100)	64.53	50.78	33.25	53.39	59.74	52.49	52.36
Balanced	Linear	64.53	50.73	33.25	53.39	59.74	52.49	52.36
	Linear (MF)	64.53	50.74	33.25	53.39	59.74	52.49	52.36
	MLP	64.53	51.01	42.46	53.39	59.74	52.38	53.92
	MLP (MF)	64.53	50.76	33.25	53.39	59.74	52.49	52.36
	Graph (k=10)	64.53	50.78	34.02	53.39	59.74	58.34	53.47
	Graph (k=100)	65.38	41.45	29.23	53.39	59.74	53.58	50.46
	Attn (k=10)	67.40	50.12	33.94	56.00	59.74	51.91	53.19
	Attn (k=100)	60.53	50.73	41.61	55.58	84.10	51.49	57.34
	D-Attn (k=10)	84.52	49.94	58.29	52.09	84.10	52.06	63.50
	D-Attn (k=100)	73.40	50.54	33.11	54.44	54.37	54.42	53.38
	kNN (k=10)	64.52	50.45	36.19	54.98	59.74	52.48	53.06
	kNN (k=100)	64.52	50.63	33.17	53.39	59.74	52.48	52.32
Low-Cost	Linear	64.52	50.59	33.17	53.39	59.74	52.48	52.32
	Linear (MF)	64.52	50.59	33.17	53.39	59.74	52.48	52.32
	MLP	64.52	50.85	39.96	53.39	59.74	52.27	53.46
	MLP (MF)	64.52	50.60	33.17	53.39	59.74	52.48	52.32
	Graph (k=10)	64.52	50.63	33.17	53.39	59.74	52.47	52.32
	Graph (k=100)	64.80	50.63	32.94	53.39	59.74	56.43	52.99
	Attn (k=10)	64.52	49.12	36.63	56.35	59.74	55.65	53.67
	Attn (k=100)	67.30	50.56	37.67	53.33	59.74	58.24	54.47
	D-Attn (k=10)	64.76	49.57	37.19	53.50	59.74	52.21	52.83
	D-Attn (k=100)	63.64	59.87	56.93	53.91	59.74	54.80	58.15

Table D.3: Utility scores on a range of text routing benchmarks. All methods directly select the optimal routing model without explicitly estimating the utility scores. Higher is better.

		AlpacaEval			HELM-Lite			OpenLLM		
		OpenAI	Claude	Mistral	OpenAI	Claude	Google	LLaMA3	Qwen2.5	Yi1.5
High-Performance	kNN (k=10)	57.72	53.38	27.61	49.83	45.23	49.56	39.81	32.12	34.61
	kNN (k=100)	58.03	53.38	26.81	49.00	42.09	48.69	39.30	25.36	33.19
	Linear	58.01	53.38	33.24	48.57	42.23	48.76	39.03	24.73	33.20
	Linear (MF)	57.85	53.38	33.29	48.66	42.81	48.87	39.17	25.19	33.25
	MLP	55.33	53.38	33.22	49.38	45.76	48.93	39.78	26.65	34.44
	MLP (MF)	58.29	53.38	33.26	48.69	43.86	48.83	39.19	24.99	33.34
	Graph (k=10)	57.82	53.38	33.21	48.86	41.42	48.59	39.34	24.35	33.19
	Graph (k=100)	58.03	53.38	33.23	48.65	45.39	51.10	37.41	21.57	33.36
	Attn (k=10)	57.16	53.38	33.27	49.06	43.61	48.85	40.20	24.95	35.46
	Attn (k=100)	58.03	53.38	33.23	49.47	45.09	49.94	38.97	21.57	33.40
Balanced	D-Attn (k=10)	57.16	53.38	33.27	47.84	42.61	48.45	39.95	26.89	38.72
	D-Attn (k=100)	55.57	53.38	33.23	47.90	42.42	49.34	39.33	22.43	33.45
	kNN (k=10)	32.41	44.93	23.23	49.76	45.03	49.45	37.31	23.15	32.66
	kNN (k=100)	34.23	51.11	25.34	48.92	41.88	48.64	37.09	21.63	32.16
	Linear	54.88	51.31	30.98	48.53	42.08	48.68	38.48	24.40	32.19
	Linear (MF)	54.85	51.31	30.97	48.58	42.42	48.72	38.61	24.85	32.24
	MLP	51.19	51.31	30.29	49.24	45.45	49.04	39.16	26.23	33.39
	MLP (MF)	54.91	51.31	30.98	48.58	43.46	48.70	38.63	24.65	32.33
	Graph (k=10)	54.88	51.31	30.98	48.87	43.95	48.55	38.50	25.69	32.22
	Graph (k=100)	54.88	51.31	30.98	50.14	44.20	51.21	38.80	21.82	32.26
Low-Cost	Attn (k=10)	54.24	51.31	30.98	48.05	41.96	47.75	38.47	25.11	33.64
	Attn (k=100)	53.39	51.31	30.98	48.88	44.68	48.77	38.66	24.62	32.25
	D-Attn (k=10)	53.51	51.31	30.98	48.04	42.23	48.42	39.64	25.09	37.36
	D-Attn (k=100)	54.31	51.31	30.98	49.71	38.01	47.86	38.46	24.97	32.32
	kNN (k=10)	24.83	27.82	20.31	49.66	44.30	49.42	36.44	21.56	31.20
	kNN (k=100)	21.41	27.47	19.49	48.88	41.60	48.57	36.29	20.84	30.91
	Linear	50.93	48.72	28.66	48.49	42.08	48.62	37.78	24.00	30.93
	Linear (MF)	50.93	48.72	28.62	48.53	42.47	48.61	37.92	24.43	30.97
	MLP	45.91	48.72	28.06	49.28	44.90	48.87	38.40	25.71	32.08
	MLP (MF)	50.93	48.72	28.63	48.52	43.32	48.63	37.93	24.23	31.06
	Graph (k=10)	50.85	48.72	28.66	48.79	43.95	48.50	37.62	24.11	30.94
	Graph (k=100)	50.93	48.72	28.66	52.62	44.28	49.85	36.02	21.69	30.64
	Attn (k=10)	50.85	48.72	28.49	48.24	40.68	47.51	37.90	24.50	32.18
	Attn (k=100)	50.69	48.72	28.66	49.03	43.16	48.79	37.89	24.08	36.13
	D-Attn (k=10)	50.85	48.72	28.49	52.00	41.35	48.13	38.35	24.25	35.63
	D-Attn (k=100)	50.77	48.72	28.66	49.24	41.86	48.60	36.07	24.41	37.56

Table D.4: Utility scores for vision language benchmark using selection based routing. Higher is better.

		Blink		Flickr30k		MathVista		MME		MMMU	
		OpenAI	Claude	OpenAI	Claude	OpenAI	Claude	OpenAI	Claude	OpenAI	Claude
High-Performance	kNN (k=10)	60.51	72.26	57.11	49.31	37.58	26.09	78.23	69.50	52.10	50.46
	kNN (k=100)	54.60	72.26	56.45	49.57	23.40	24.71	74.76	69.50	46.36	49.71
	Linear	57.04	72.26	56.45	53.03	23.40	25.42	72.21	72.92	46.36	49.71
	Linear (MF)	63.99	72.26	56.45	46.64	32.62	31.02	78.00	76.99	46.74	50.85
	MLP	66.06	75.68	57.73	54.64	42.54	33.81	74.06	81.25	54.40	53.07
	MLP (MF)	65.38	72.26	56.45	47.54	23.40	33.86	75.91	79.69	46.36	49.71
	Graph (k=10)	54.60	72.26	56.45	46.50	34.03	26.12	73.83	73.37	46.36	49.71
	Graph (k=100)	54.30	73.58	48.02	61.94	25.47	27.17	69.67	79.13	45.15	51.96
	Attn (k=10)	60.98	72.60	56.51	62.30	35.37	31.89	77.25	88.02	53.96	52.28
	Attn (k=100)	61.38	71.38	56.06	54.94	43.92	50.58	67.66	83.94	47.12	50.09
Balanced	D-Attn (k=10)	55.30	71.75	51.62	61.90	41.01	36.24	55.73	88.02	48.48	51.51
	D-Attn (k=100)	63.96	72.56	48.02	52.66	29.77	50.58	72.36	85.73	45.58	49.27
	kNN (k=10)	60.48	71.22	56.97	47.15	35.42	24.26	77.03	67.87	52.08	49.31
	kNN (k=100)	54.58	71.22	56.37	47.29	23.39	24.26	73.33	67.87	46.35	49.31
	Linear	57.01	71.22	56.37	51.53	23.39	24.96	72.17	71.07	46.35	49.31
	Linear (MF)	63.96	71.22	56.37	45.48	32.60	30.30	77.95	74.78	46.73	50.44
	MLP	65.97	73.68	56.77	51.59	42.47	32.90	74.02	78.47	54.35	52.31
	MLP (MF)	65.35	71.22	56.37	46.06	23.39	33.13	75.87	77.17	46.35	49.31
	Graph (k=10)	55.10	71.03	56.37	53.52	29.05	24.26	71.71	75.01	45.96	48.84
	Graph (k=100)	54.52	71.61	58.28	49.86	33.77	39.33	70.76	78.30	45.21	53.20
Low-Cost	Attn (k=10)	62.51	70.98	57.25	56.62	44.50	24.77	78.27	79.73	48.40	52.11
	Attn (k=100)	59.45	72.36	57.09	56.76	40.86	24.86	75.87	78.80	46.00	49.30
	D-Attn (k=10)	62.50	71.85	56.71	56.55	26.45	28.19	90.22	83.60	48.79	52.20
	D-Attn (k=100)	55.53	71.28	56.90	56.63	36.05	48.62	69.26	78.19	52.68	49.57
	kNN (k=10)	60.27	69.92	56.55	46.03	30.43	23.71	76.97	65.84	52.05	48.81
	kNN (k=100)	54.54	69.92	56.28	45.69	23.38	23.71	73.27	65.84	46.34	48.81
	Linear	56.98	69.92	56.28	48.62	23.38	24.39	72.12	68.76	46.33	48.81
	Linear (MF)	63.93	69.92	56.28	47.14	32.57	29.39	77.90	72.01	46.71	49.92
	MLP	65.86	71.19	55.35	48.31	42.38	31.76	73.96	74.99	54.30	51.35
	MLP (MF)	65.31	69.92	56.28	45.35	23.38	32.23	75.81	74.02	46.34	48.81
	Graph (k=10)	54.71	69.92	56.28	46.05	33.25	23.71	73.73	69.41	46.34	48.81
	Graph (k=100)	65.37	69.92	57.73	50.17	41.66	32.67	67.08	71.99	46.86	50.36
	Attn (k=10)	62.53	70.31	56.88	50.33	37.42	27.98	77.17	79.41	60.31	50.20
	Attn (k=100)	57.20	70.65	56.81	48.47	40.05	26.17	77.10	73.93	45.24	49.16
	D-Attn (k=10)	62.69	67.35	57.54	50.12	23.80	24.83	89.63	79.62	45.85	50.09
	D-Attn (k=100)	59.16	70.43	56.71	47.78	23.35	46.17	79.86	71.47	49.04	51.28